J. Plasma Physics (2006), *vol.* 72, *part* 6, *pp.* 1299–1302. © 2006 Cambridge University Press
doi:10.1017/S0022377806005599 Printed in the United Kingdom

Vlasov simulations of trapping and inhomogeneity in Raman scattering

D. J. STROZZI,[1,3]
M. M. SHOUCRI,[2] A. BERS,[1] E. A. WILLIAMS[3]
and A. B. LANGDON[3]

[1]Massachusetts Institute of Technology, Cambridge, MA 02139, USA
[2]Institut de Recherche de l'Hydro Québec, Varennes, Qc J3X1S1, Canada
[3]Lawrence Livermore National Laboratory (LLNL), Livermore, CA 94550, USA
(dstrozzi@llnl.gov)

(Received 15 August 2005 and accepted 23 November 2005)

Abstract. We study stimulated Raman scattering (SRS) in laser-fusion plasmas with the Eulerian Vlasov code ELVIS. Backward SRS occurs in sub-picosecond bursts and far exceeds linear theory. Forward SRS and re-scatter of backward SRS are also observed. The plasma wave frequency downshifts from the linear dispersion curve, and the electron distribution flattens. This is consistent with trapping and reduces Landau damping. There is some acoustic ($\omega \propto k$) activity and possibly stimulated electron acoustic scatter. Kinetic ions do not affect SRS for early times but suppress it later on. SRS from inhomogeneous plasmas exhibits a kinetic enhancement for long density scale lengths. More scattering results when the pump propagates towards a higher as opposed to towards a lower density.

1. Introduction and code model

Laser–plasma interactions must be controlled for inertial fusion to succeed. This paper examines stimulated Raman scattering (SRS), or the parametric coupling of a pump light wave (the laser, mode 0) to a daughter light wave (mode 1) and an electron plasma-wave (EPW, mode 2). Kinetic effects, such as electron trapping, in the daughter EPW are seen to be important in backward SRS (BSRS). One-dimensional (1D) kinetic simulations presented here show BSRS much greater than coupled-mode theory for both homogeneous and inhomogeneous plasmas [1]. Strong nonlinearity and non-thermal electron distributions result.

ELVIS [2] is a 1D Eulerian Vlasov code that evolves the distribution function f_s ($s =$ species; e for electrons) on a fixed phase-space grid. It uses operator splitting for the time advance [3, 4] and cubic spline interpolation for shifting f_s in position (x) and momentum (p_x). Light waves are linearly polarized in y. The ions can be immobile or kinetic. The governing equations are

$$[\partial_t + (p_x/m_s)\partial_x + (Z_s e)\,(E_x + v_{ys}B_z)\,\partial_{p_x}]\,f_s = \nu_{\mathrm{K}s}\,(x)\,(n_s \hat{f}_{0s} - f_s), \tag{1.1}$$

$$\partial_x E_x = \frac{e}{\varepsilon_0}\sum_s Z_s n_s, \quad m_s \partial_t v_{ys} = e Z_s E_y, \tag{1.2}$$

$$(\partial_t \pm c\partial_x)\,E^{\pm} = -\frac{e}{\varepsilon_0}\sum_s Z_s n_s v_{ys}, \qquad E^{\pm} \equiv E_y \pm cB_z. \tag{1.3}$$

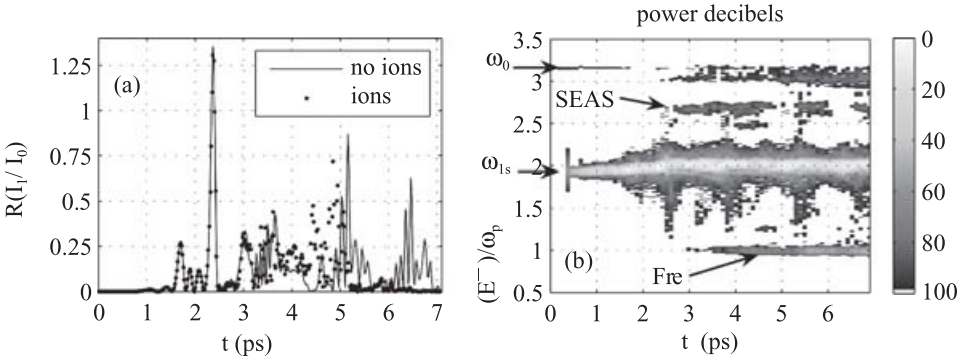

Figure 1. (a) Reflectivity for a homogeneous run with immobile (solid curve) and kinetic ions (dotted curve). (b) Spectrum of reflected light for immobile ions. 'Fre' and 'SEAS' label BSRS re-scatter and possible stimulated electron acoustic scattering.

$m_s, Z_s e$ ($e > 0$) are the species mass and charge. A number-conserving Krook relaxation operator is included, with relaxation rate $\nu_{Ks}(x)$ and equilibrium Maxwellian $\hat{f}_{0s}$ ($\int dp\ \hat{f}_{0s} = 1$). We use a large $\nu_{Ks} \sim 0.2\omega_p$ ($\omega_p^2 = n_0 e^2/(\epsilon_0 m_e)$) at the edges of the finite length density profile to absorb plasma waves generated by SRS and prevent their reflection. A non-zero central value of ν_{Ks} can mimic sideloss from a laser speckle. We advance $E^{\pm}$ without dispersion (in vacuum) by shifts of one x gridpoint, which imposes $dx = c\ dt$.

2. Simulation results

We simulate a pump laser with $\lambda_0 = 351\,\text{nm}$ (vacuum) and intensity $I_0 = 2 \times 10^{15}\,\text{W cm}^{-2}$ impinging from the left (E^+ contains the pump) on a finite length plasma with a flat central region $75.1\,\mu\text{m}$ wide of density $n_0 = 0.1 n_c$ (critical density $n_c = n_0\omega_0^2/\omega_p^2$) and temperature $T_e = 3$ keV. Since Vlasov codes are low-noise there are no numerical fluctuations for SRS to grow from. We therefore inject a counter-propagating seed light wave via E^- with $\lambda_{1s} = 574\,\text{nm}$ and $I_1 = 10^{-5} I_0$. This light has the maximum linear BSRS growth rate and couples to an EPW with $k_2\lambda_D = 0.357$ and a Landau damping rate $\nu_2 = 0.038\omega_p$ ($\lambda_D = v_{Te}/\omega_p$, $v_{Te}^2 = T_e/m_e$). The x and p_x grid spacings are $dx = 0.880\lambda_D$ and $dp = 0.0437 v_{Te} m_e$. Linearly, BSRS is convective with amplitude gain rate $\alpha = 0.019\,\mu\text{m}^{-1}$, giving a reflectivity $R_{\text{lin}} = 1.72 \times 10^{-4}$. The numerical R, shown as the solid curve in Fig. 1(a), is well above this level. R comes in sub-picosecond bursts and has a time average from 1 ps to the run end of $R_{\text{av}} = 13.8\%$. $\nu_{Ks} \neq 0$ only at the edges. Repeating the run with a non-zero central ν_{Ks} shows a sharp cutoff of the reflectivity for $\nu_{Ks} \gtrsim 10^{-3}\omega_p$.

The streaked spectrum of reflected light E^- at the left edge is shown in Fig. 1(b). Almost all of the energy is contained in BSRS. $\omega_{1s} = 1.93\omega_p$ is the seed light frequency. Initially BSRS occurs at ω_{1s} but upshifts for $t \gtrsim 2$ ps, corresponding to a downshift in ω_2. The weak signal near ω_p labeled 'Fre' is the forward Raman re-scatter of upshifted BSRS light. The longitudinal E_x spectrum in Fig. 2(a) reveals the plasma wave at the matching k and ω. Re-scatter is only possible due to the upshift in ω_1, since $\omega_p > \omega_{1s}/2$. The feature slightly above $2.5\omega_p$, labeled SEAS (stimulated electron acoustic scatter), may be scattering off the acoustic longitudinal activity discussed below [6]. The transmitted light (E^+) spectrum (not shown) exhibits for $t \gtrsim 3$ ps weak levels of both forward SRS (FSRS) and the anti-Stokes line ($\omega = \omega_0 + \omega_p$) of the pump, even though neither is seeded.

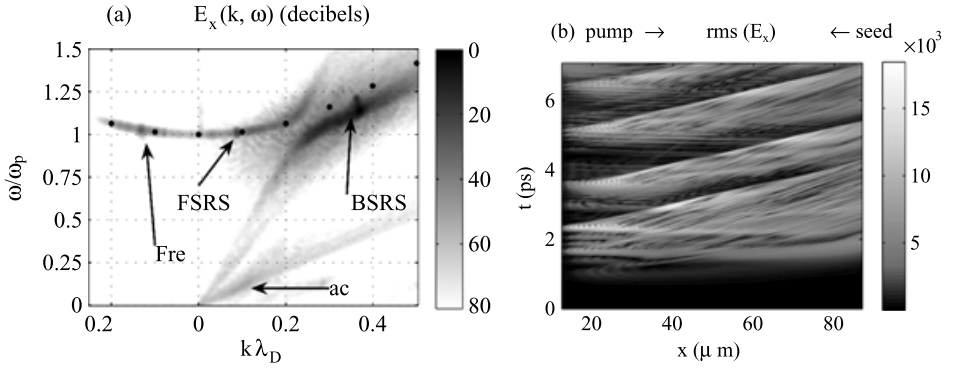

Figure 2. (a) $E_x(k,\omega)$ spectrum for homogeneous, immobile ions run. 'Fre' and 'ac' label BSRS re-scatter and acoustic activity. The black dots are the linear EPW dispersion curve. (b) Root-mean-square averaged $E_x(x,t)$.

The longitudinal electric field spectrum $E_x(k,\omega)$ in Fig. 2(a) reveals that the BSRS plasma-wave activity is downshifted in frequency from the linear dispersion curve. This is qualitatively consistent with the frequency downshift due to electron trapping [7], and larger frequency downshift occurs during periods when larger EPW amplitudes are observed. The downshifted EPW connects with a weak acoustic feature ($\omega \propto k$) that extends to $\omega = 0$. There is a stronger, lower phase velocity ($v_\mathrm{p} \approx 1.3 v_\mathrm{Te}$) acoustic mode, which satisfies phase matching for the SEAS reflected light seen in Fig. 1(b). This mode's phase velocity agrees with the acoustic mode studied by Rose and Russell in [5]. In addition, plasma waves corresponding to FSRS and re-scatter of BSRS occur on the EPW dispersion curve. Figure 2(b) presents the x and t root mean square averaged $E_x(x,t)$, which shows the EPWs occur as a series of wide pulses that move parallel to the pump. The group velocity matches the slope of the BSRS plasma waves. Near the laser entrance some pulses propagate opposite the laser.

The electron distribution f_e forms phase-space vortices at the EPW phase velocity $v_\mathrm{p2} = \omega_2/k_2$ ($0.264c$ linearly). The space-averaged $\langle f_\mathrm{e} \rangle$, displayed in Fig. 3(a), is flattened due to trapping in this region. Landau damping ($\sim \partial f_\mathrm{e}/\partial p_x$) is greatly reduced by flattening, which thereby enhances the reflectivity [8]. When the EPW amplitude is large f_e is quite flat, and only for brief periods ($\lesssim 0.1$ ps) do we see a small bump (region of $\partial \langle f_\mathrm{e} \rangle / \partial p_x > 0$) form slightly above v_p2.

The run was repeated with kinetic helium ions ($m_\mathrm{i} = 4m_\mathrm{p}$, $T_\mathrm{i} = 750$ eV, $Z_\mathrm{i} T_\mathrm{e}/T_\mathrm{i} = 8$) and yielded the dotted R in Fig. 1(a). Early in time, R is the same for immobile and kinetic ions, while for the last 2 ps it is very low with kinetic ions. We do not see evidence of Langmuir decay instability (EPW → EPW + IAW (ion acoustic wave)) of the EPW or stimulated Brillouin scattering (photon → photon + IAW) of the pump. Instead, very high E_x activity develops on the left edge of the box around $t = 5$ ps, involving large ion density fluctuations; BSRS is minimal after this. Further study of the role of ions is underway.

In an inhomogeneous medium, where the wave k's vary in space, the k matching condition $k_0 = k_1 + k_2$ for a three-wave interaction is only satisfied at one point. Away from this point, dephasing limits the interaction. We performed simulations for the same parameters as the homogeneous run with kinetic ions discussed above. However, the central region of the density profile now has a linear gradient extending for $100\,\mu$m. We vary the endpoint densities and thereby change the density

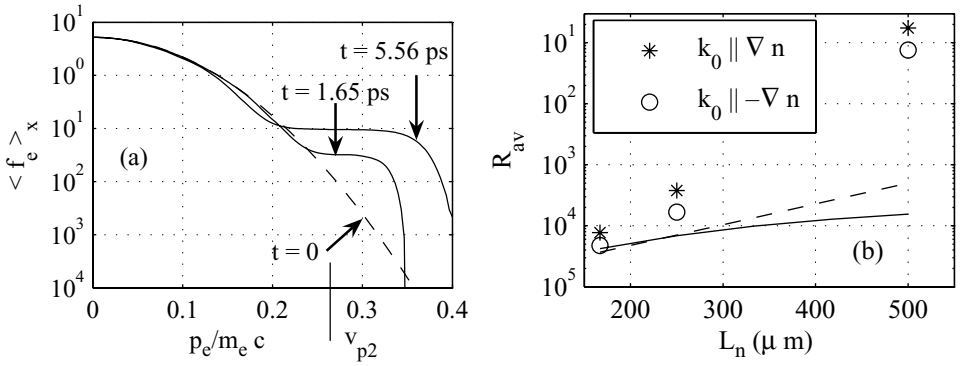

Figure 3. (a) Space-averaged f_e over central 5.62 μm of box for homogeneous, immobile ions run. (b) Average reflectivity for inhomogeneous runs with $L_n = (167, 250, 500)\mu$m. (Solid, dashed) curves are the coupled-mode (strong damping limit, Rosenbluth undamped) steady-state R.

scale length $L_n = n/(dn/dx)$. The reflectivities for several L_n are shown in Fig. 3(b), for the pump propagating towards higher and lower densities. Also plotted is the steady-state R predicted from coupled-mode theory, solved in the strong EPW damping limit (solid curve) as well as the Rosenbluth undamped result (dashed curve). R is independent of pump propagation direction for both coupled-mode calculations, yet the simulations consistently show higher R for $\mathbf{k}_0 || \nabla n$. We are formulating a theory to explain the high R and the role of pump propagation direction.

3. Conclusions

Vlasov simulations of SRS show strong enhancement of the scattering over coupled-mode predictions for both homogeneous and inhomogeneous plasmas. The resulting plasma waves do not satisfy the linear dispersion relation. The electron distribution shows large trapping and flattening. SEAS may be present. The roles of sideloss and ions need to be further examined, and analytic models that explain these findings need to be developed.

Acknowledgements

This work was supported by the US Department of Energy under grant No. DE-FG02-91ER54109 at MIT and under contract No. W-7405-ENG-48 at LLNL.

References

[1] Strozzi, D. 2005 *Ph.D Thesis*, Department of Physics, MIT.
[2] Strozzi, D., Shoucri, M. and Bers, A. 2004 *Comput. Phys. Comm.* **164**, 156–159.
[3] Cheng, C. Z. and Knorr, G. 1976 *J. Comput. Phys.* **22**, 330–351.
[4] Ghizzo, A. et al. 1990 *J. Comput. Phys.* **90**, 431–457.
[5] Rose, H. A. and Russell, D. 2001 *Phys. Plasmas* **8**, 4784–4799.
[6] Montgomery, D. S. et al. 2001 *Phys. Rev. Lett.* **87**, 155001.
[7] Morales, G. J. and O'Neil, T. M. 1972 *Phys. Rev. Lett.* **28**, 417–420.
[8] Vu, H. X., DuBois, D. F. and Bezzerides, B. 2002 *Phys. Plasmas* **9**, 1745–1763.